Lasers in Surgery and Medicine 24:103–112 (1999)

Effects of Overlap and Pass Number in CO_2 Laser Skin Resurfacing: A Study of Residual Thermal Damage, Cell Death, and Wound Healing

E. Victor Ross, MD, CDR, MC, USN,[1,2]* David J. Barnette, MD, CAPT, MC, USN,[2] Robert D. Glatter, MD,[1] and Joop M. Grevelink, MD, PhD[1]

[1]Dermatology Laser Center and Wellman Laboratories of Photomedicine, Massachusetts General Hospital, Boston, Massachusetts 02114
[2]Department of Dermatology, Naval Medical Center San Diego, San Diego, California 92134

Background: **Newer CO_2 laser systems incorporating short pulse and scanning technology have been used effectively to resurface the skin. As the number of resurfacing cases has increased, hypertrophic scarring has been reported more commonly. Previous dermabrasion and continuous wave CO_2 studies have suggested that depth of injury and thermal damage are important predictors of scarring for a given anatomic region. To determine whether rapid overlapping of laser pulses/scans significantly altered wound healing, we examined residual thermal damage, cell death, and histologic and clinical wound healing in a farm pig.**
Methods and Materials: **Two popular CO_2 systems were used, with a range of radiant exposures, degrees of overlap, and numbers of passes. Thermal damage was assessed by histology, and dermal cell viability was measured with nitrotetrazolium blue staining. Presence or absence of clinical scarring was determined by textural change and loss of skin markings.**
Results: **We observed that dermal thermal damage did not increase significantly with pass number when performed as in the normal clinical setting (for 2–4 passes); however, by delivering rapidly overlapping pulses and scans, residual thermal damage and cell death depth were increased as much as 100% over areas without immediate overlap of laser impacts.**
Conclusions: **Immediate overlapping of CO_2 laser pulses and scans is a significant risk factor in increasing thermal damage, cell death, and possibly scarring. Lasers Surg. Med. 24:103–112, 1999.** **Published 1999 Wiley-Liss, Inc.†**

Key words: time constant; critical frequency; transition zone; scarring; thermal relaxation time

INTRODUCTION

Creative clinical applications of laser technology have expanded the role of pulsed and rapidly scanned CO_2 lasers in dermatology. Over the past 5 years, CO_2 lasers have been widely promoted for smoothing skin irregularities, and the relative safety of laser skin resurfacing (LSR) has been attributed to minimization of thermal damage [1–9]. Although designs of newer generation

Preliminary results were published in *Lasers in Surgery: Advanced Characterization, Therapeutics, and Systems VII,* Anderson RR, MD, et al. editors. Proc. SPIE 2970, 395–405 (1997). Results were also presented at the annual meeting of the American Society for Laser Medicine and Surgery, Phoenix, AZ, April 1997.

*Correspondence to: E. Victor Ross, M.D., Box 324, Naval Medical Center San Diego, 34800 Bob Wilson Drive, San Diego, CA 92134. E-mail: vross@snd10.med.navy.mil

Accepted 19 October 1998

CO_2 lasers permit less operator dependence than, for example, dermabrasion, where subtle hand movements often determine efficacy and safety, recent anecdotal reports of laser resurfacing-induced scarring are a source of concern. One potential cause is rapid overlapping of scans or pulses in a machine-gun manner. The subsequent superposition of laser exposures might allow for cumulative tissue heating such that thermal damage is considerably increased. To determine the potential role of pulse or scan stacking (immediate overlapping of pulses or scans) in thermal damage and scarring, we measured residual thermal damage in a live pig with two popular resurfacing lasers. In addition, the wounds were assessed at several time intervals after the day of surgery.

METHODS AND MATERIALS

Lasers

One of the two systems in this study was a 40-W continuous wave (CW) CO_2 laser (Model 40C, Sharplan, Allendale, NJ) coupled to the SilkTouch optomechanical flashscanner. This scanner uses two almost, but not exactly, parallel mirrors to produce a fine spiral beam (approximately 400 μm in diameter for the 6-mm scan size) whose dwell time is approximately 1 msec [10]. There are roughly 16–18 concentric tracks across the entire scan diameter (personal communication with M. Slatkine, Ph.D., Sharplan Laser). By laying down concentric adjacent spirals, a full scan is produced. Parameters that are set by the operator include the laser power, the laser "on" time, and the laser "off" time. A standard scan is completed in 0.2 sec (standard "on" time), after which the operator is allowed a certain time to move the handpiece to an adjacent spot. This "off" time is set to allow for a comfortable hand movement rate [7]. The total fluence per pass with the SilkTouch is determined as follows:

$$\begin{aligned}\text{fluence} &= \text{power density} \times \text{time} \\ &= (\text{CW power/beam area}) \times (\text{dwell time}) \\ &= \text{J/cm}^2.\end{aligned}$$

Now, let power P = 16 W (typical power setting), beam diameter = 400 μm (or 4×10^{-4} cm), and the dwell time = 1 msec, then the fluence

$$\begin{aligned}&= \left(\frac{16\ \text{W}}{\pi(0.02\ \text{cm})^2}\right) * (0.001\ \text{sec}) \\ &\approx 13\ \text{J/cm}^2.\end{aligned}$$

The other laser used in this study was the UltraPulse 5000C (Coherent, Palo Alto, CA), a high-energy pulsed system with pulse duration of approximately 500–800 μs. The laser was configured with the computer pattern generator (CPG), a proprietary XY scanner capable of producing multiple 2.25-mm-diameter impacts at a rate of up to 200 Hz. Other than repetition rate, two operator-determined parameters are pulse energy and density. Density refers to the degree of overlap between adjacent pulses with the CPG. A density of 4, for example, sets the overlap at 20%, whereas densitites of 6 and 9 set the overlap at 35% and 60%, respectively [11]. Most clinicians have found that the CPG can be used safely with densities of 4, 5, and 6 so long as other laser parameters and numbers of passes are appropriate for the specific anatomic location and application [1, 12, 13]. In addition to setting the distance between individual pulses within a scan, the clinician can select the scan repetition rate, defined as the interval between successive entire scans. This is the time the physician has to move the scanner to an adjacent area. In this manner, the skin is treated in the same manner as laying down tile on a floor. The fluence is calculated with the UltraPulse simply by taking the pulse energy and dividing by the spot area. For example, for a 300-mJ pulse and 2.25-mm spot (area = 0.4 cm^2), the average fluence is 7.5 J/cm^2.

Animal

An intramuscular injection of ketamine (20 mg/kg) was used to initiate anesthesia in a farm pig (*Sus scrofa domesticus*). Anesthesia was induced and maintained with halothane and nitrous oxide. The flank hair was clipped with electric shears and shaven, after which the skin was prepped with chlorhexidine solution. Two weeks prior to surgery, the pig was tattooed to demarcate square-shaped laser sites (2 × 2 cm each). One-half of the treatment sites were used for follow-up of the gross wounds; the other half was used for biopsies. Each tattoo site was photographed with a Polaroid camera (Model CU5 Land camera, Cambridge, MA) with a fixed image:object size ratio (2:1) before and after irradiation. Bacitracin ointment and sterile bandages were placed on the treated areas daily for 3 days, after which the areas were left open to air. No chemical or mechanical debridement was performed. The animal was taken back to the operating room for biopsies, photographs, and clinical

TABLE 1. Laser Settings for SilkTouch Scan Sites

Site	Power (W)	Cooling time between passes	No. of passes	Scanner settings		
				On time (sec)	Off time (sec)	Scan size (mm)
1	16	2 min	3	0.2	0.4	6
2	16	2 min	4	0.2	0.4	6
3	16	0.4 sec	1 + 2	0.2	0.2	6
4	16	0.4 sec	1 + 3	0.2	0.2	6
5	16	0.2 sec	1 + 3	0.6	0.0	6

TABLE 2. Laser Settings for UltraPulse With the Computer Pattern Generator

Site	Pulse energy (mJ)	Density	No. of passes	Spot size (mm)	Scan size (mm)	Scans stacked at 2 Hz	Cooling time between overlapping scans (msec)	Repetition rate for individual pulses within scan (Hz)	Cooling time between overlapping portions of adjacent spots within scan (msec)
6	300	3	3	2.25	15 × 15	No	N/A[a]	200	4
7	300	6	3	2.25	15 × 15	No	N/A	200	4
8	300	9	3	2.25	15 × 15	No	N/A	200	4
9	300	3	3	2.25	15 × 15	Yes	500	200	4
10	300	6	3	2.25	15 × 15	Yes	500	200	4
11	300	9	3	2.25	15 × 15	Yes	500	200	4

[a]N/A, not applicable.

assessment on posttreatment days 1, 5, 21, and 42.

Procedure

The laser scans and pulse settings are outlined in Tables 1 and 2. Settings were configured according to those typically used in clinical practice. "Pass" refers to the number of times any focal region was irradiated. Details of the laser procedures are as follows.

The SilkTouch scanner was used first as recommended in clinical practice (sites 1–2, Table 1) by laying down each scan precisely adjacent to each other with no immediate overlap, and wiping with wet gauze between passes. The next three 2- × 2-cm squares (sites 3–5) were treated in such a way as to mimic potential "mistakes" in clinical practice. First, a pass was made in the usual fashion with no contiguous overlap of 0.2-sec scans. After wiping, the epidermis was removed with this pass. Next, however, rather than using the laser as in standard practice, we reset the off time to 0.2 sec and deliberately held the handpiece in a constant position, performing two immediate overlapping scans for site 3 and three for site 4, respectively. Therefore, the handpiece was held in place for 0.6 sec (on–off–on) for site 3 and 1.0 sec for site 4 (on–off–on–off–on) before moving the handpiece to the adjacent spot. For site 5, after a first normal pass (with post-pass wiping with wet gauze), we deliberately set the on time so that three successive scans would be applied with zero off time. In this case, the on time was set to 0.6 sec, after which the handpiece was moved to an adjacent spot in the usual fashion.

For the UltraPulse laser (sites 6–8), square scans were applied adjacent to each other with no overlap. For each scan pass, 49 equidistant pulses were applied at 200 Hz so that 0.25 sec was required to complete a scan. Each site received three passes as in standard practice (wounds wiped with wet gauze after each pass, and approximately a 2-min interval between successive passes). With this laser system for sites 6–8, the scanner controlled the degree and rapidity of overlap. Because the laser fires for ~1 msec per pulse, the laser was on roughly 20% of the time, leaving approximately 4 msec between adjacent pulses.

For sites 9–11, after a normal first pass was made to remove the epidermis, two overlapping additional passes were made with intervals of 0.5 sec.

In addition, three sites were treated with parameters as presented in Table 4. At these sites, 2, 3, and 4 passes were performed in the usual manner, with wiping and considerable time between passes (>1 min). This allowed us to assess

the effect of pass number alone, independent of stacking.

Histology

Three sets of biopsies were obtained just after irradiation from all treatment sites. These were rectangular full-thickness specimens (approximately 6 × 15 mm at the surface) that included treated and normal skin. The specimens were fixed in formalin, cut longitudinally, embedded in paraffin, and stained with hematoxylin and eosin (H&E). Additional biopsies of this type were obtained postoperatively after 1, 5, 21, and 42 days. Immediate postoperative specimens were viewed microscopically with an eyepiece reticle, and the average depth of thermally altered collagen from 10 sites along the length of the specimen was recorded. Two distinct zones were noted by tinctorial changes. Most superficially, a well-demarcated band of basophilic staining collagen was observed. This band represents the zone of residual thermal damage usually referred to in the literature as the coagulative zone (Z_{coag}). Deep to this zone, a layer of hypereosinophilic staining was noted, with fibroblast nuclei showing hyperchromasia and pyknosis (transition zone = Z_{tr}). For biopsies from postoperative day 1, the depth polymorphonuclear leukocytes (PMNs) margination was measured. This was taken to be the deepest extent to which PMNs formed a "picket fence" at the base of the wound, as measured from the tissue surface. This also corresponded roughly to the depth of fibroblast necrosis (as assessed by cytology, where live fibroblasts showed normal nuclear morphology). The histologic depths of thermal damage and fibroplasia depths for each time internal were compared by analysis of variance with the Tukey post hoc test for each laser system (significance set at $P < 0.05$).

Dermal ablation depths were measured for representative nonstacked sites (Table 4) by measuring the heights of residual papilla and adjacent untreated dermis within the same specimens (measuring the "step-off"). Ten measurements were made across each of the specimens. The ablation depths were measured primarily to confirm that ablation was minimal for the range of fluences used in the experiment, that is, that heating was essentially nonablative.

Biopsies were obtained immediately after treatment and one day postoperatively for assay for cellular lactic dehydrogenase (LDA) activity. Because only viable cells show the active enzyme, this method provides a sensitive way for determining the depth of tissue necrosis. This method uses a nitrotetrazolium (NBT) salt, a redox indicator that turns blue in the presence of lactic dehydrogenase [14]. Three 4-mm punch biopsies were obtained from each treatment site, frozen in dry ice, and stored at −75°C. Thin sections were cut (~0.5–1 mm thick) and incubated in the following medium overnight before routine processing:

1. 2.5 mg of paranitrophenyl-substituted ditetrazolium salt
2. 5 ml of Michaelis's barbital sodium acetate buffer
3. 1.5 mg β-nicatinomide adenine dinucleotide
4. 15 mg sodium lactate

For positive controls, normal nonirradiated skin was stained. For negative controls, sections were taken from skin heated to 100°C for 100 sec. After incubation, all biopsy specimens were fixed in formalin and embedded in paraffin. No counterstain was used. These sections were viewed microscopically, and the depth of nonviable tissue, as noted by the lack of NBT staining, was measured from the tissue surface with an eyepiece reticle. An average of five measurements made across the breadth of each specimen was recorded.

RESULTS

Immediately After Surgery

With the exception of slightly more yellowing with stacking, on gross examination of the skin, there were few significant differences between laser systems, numbers of passes, and laser parameters. Microscopically, two major zones of collagen denaturation could be identified (Fig. 1A, B). Superficially, a basophilic staining zone (Z_{coag}) comprised the bulk of denatured material; this zone showed complete loss of birefringence. Deep to this zone was a second, less distinct region, where collagen showed mild hypereosinophilia and partial retained birefringence, with focal amorphous areas showing a slightly bluish hue. This zone (Z_{tr}) was most extensive from sites with rapidly overlapping pulses and scans. For sites 1, 2, 6, and 7, this zone was almost imperceptible, and there was an abrupt transition from denatured to normal collagen. The number of passes (e.g., three vs. four for sites 1 and 2), in contrast to stacking, did not significantly affect the residual thermal damage level or pattern. The total depth of immediate thermal damage (incorporating Z_{coag} and Z_{tr}) is summarized for the sites in Table 3. NBT

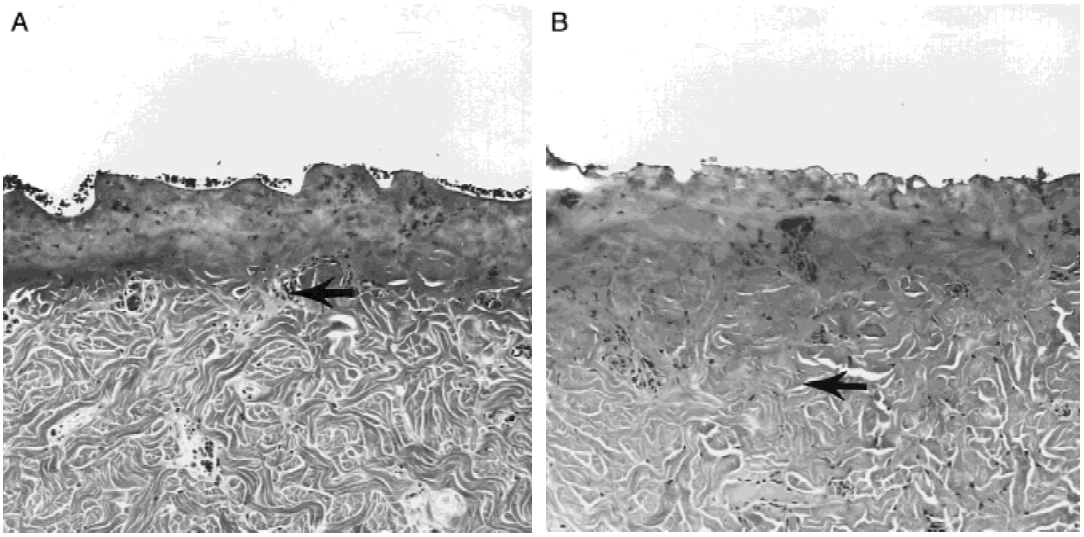

Fig. 1. **A:** Immediate thermal damage from site 1 (not stacked). Note abrupt change in collagen staining (arrow). **B:** Immediate damage from site 3 (stacked). Note deeper transition zone that extends to arrow.

TABLE 3. Thermal Damage and Depth of Necrosis

	Immediately after surgery		
Site	Depth of basophilic collagen change (μm)	Total depth (μm) of collagen change (including transition zone)	Postoperative day 1: Depth of PMN band/NBT staining (μm)[a]
1	131 ± 13	152 ± 17	196 ± 31
2	122 ± 12	160 ± 12	210 ± 24
3	136 ± 13	236 ± 31	253 ± 45
4	157 ± 15	256 ± 26	240 ± 32
5	160 ± 11	254 ± 31	310 ± 43
6	70 ± 9	108 ± 8	158 ± 37
7	95 ± 13	142 ± 13	177 ± 18
8	145 ± 20	212 ± 25	185 ± 21
9	95 ± 10	145 ± 21	155 ± 27
10	155 ± 13	210 ± 29	193 ± 40
11	195 ± 15	250 ± 31	230 ± 32

[a]PMN, polymorphonuclear; NBT, nitrotetrazolium.

stains showed cell viability beginning just below the basophilic staining collagen.

Statistically, the basophilic zones were different for the SilkTouch system between stacked and nonstacked sites (1 and 2 vs. 4 and 5). For UltraPulse sites, the differences were significant based on density (6 vs. 7 vs. 8) and scan stacking (6 vs. 9, 7 v. 10, 8 vs. 11) (Table 3). The total depths of residual thermal damage (RTD) (Z_{coag} + Z_{tr}) showed even stronger grouping based on stacking, where both SilkTouch and UltraPulse sites showed significant differences based on off times and densities (for the CPG).

One day after treatment, a serosanguinous discharge and pinpoint bleeding were noted on removal of the dressings. There were no remarkable gross differences based on pass number or degree of immediate overlap (stacking). H&E-stained sections regularly showed PMN margination at the base of the wounds. The depth of PMN infiltration (Fig. 2) coincided with the depth of necrosis as indicated by NBT staining (Fig. 3) and also coincided roughly to the depth of the hypereosinophilic zone (noted immediately postoperatively; Table 3). In some sections, there was focal sloughing of basophilic staining collagen. This sloughing typically occurred at the level of greatest density of PMNs. Deep to this zone at day 1, there were scattered inflammatory cells and pyknotic fibroblast nuclei. At sites with stack-

TABLE 4. Residual Thermal Damage (RTD) and Ablation Depths as a Function of Pass Number (Nonstacked)

	UltraPulse[a]			SilkTouch[b]		
Pass	Dermal ablation depth (μm)	Width of coagulation (μm)	Width (coagulation) + transition; μm)	Dermal ablation depth	Width of coagulation (μm)	Width (coagulation + transition; μm)
2	20	118 ± 23	134 ± 15	20	126 ± 21	145 ± 32
3	30	132 ± 27	150 ± 24	40	136 ± 13	154 ± 13
4	50	135 ± 25	158 ± 32	60	138 ± 24	152 ± 34

[a]With a computer pattern generator density of 4 and a pulse energy of 300 mJ.
[b]With 16 W, 6-mm scan, and 0.2 sec on time.

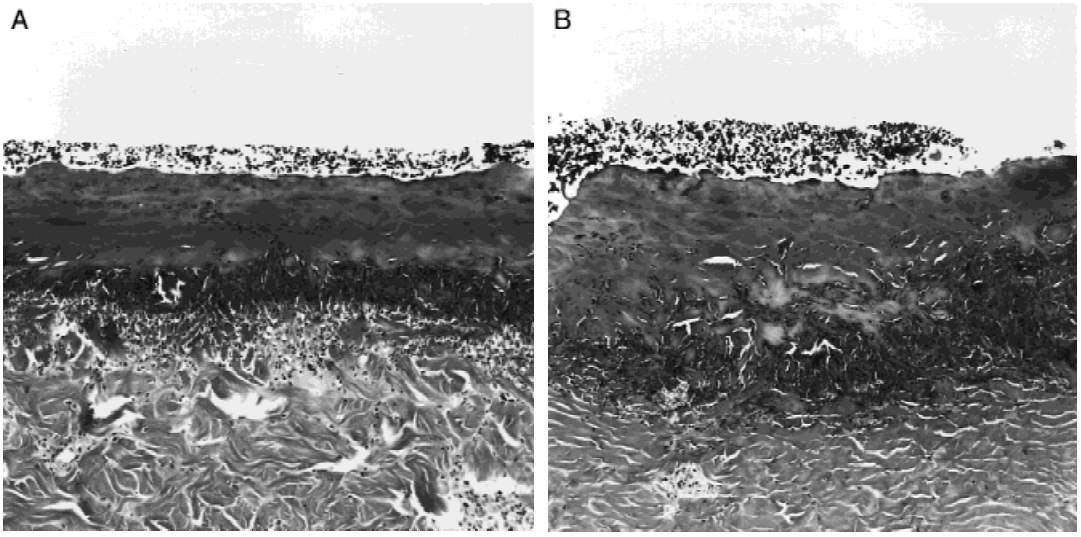

Fig. 2. **A:** Site 1, 1 day after surgery. Note the line of polymorphonuclear leukocytes (PMNs). **B:** Site 3, 1 day after surgery. Note the more extensive depth of necrosis (PMNs).

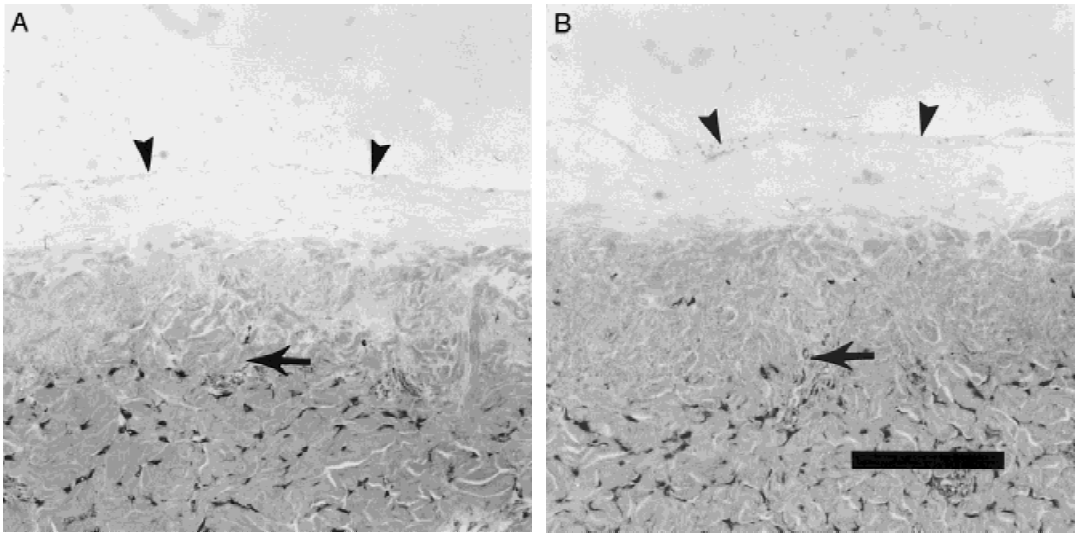

Fig. 3. **A:** Nitrotetrazolium (NBT) stain from site 1, 1 day after surgery. The unstained area (triangle marked by arrowheads and arrow in A and B) indicates area of cell death. **B:** NBT stain from site 3, 1 day after surgery. Note the increased depth of cell death. Bar = 100 μm.

ing, the band of PMNs usually extended deeper and in some cases lined up at the base of the zone of hypereosinophilic collagen (vs. the basophilic zone for nonstacked sites). Statistically, based on depths of fibroblast necrosis, the nonstacked and stacked sites were significantly different for the SilkTouch sites. In addition, site 5 was different from the other two stacked SilkTouch sites. For the UltraPulse sites, depths were significantly different as a function of density and presence or absence of scan stacking, with the exception of density 3, where stacking did not increase the depth of necrosis.

By postoperative day 5, all sites grossly showed different degrees of surface erythema and focal crusting, with stacked sites showing more intense erythema and pinpoint bleeding. Biopsies from postoperative day 5 showed partial reepithelialization in all cases. In stacked wounds, the neoepidermis appeared less developed and poorly attached to the underlying tissue with greater subsurface edema. In one section from case 4, there was a 30-μm layer of denatured collagen underlying the newly formed epidermis. This collagen appeared to be enmeshed within a band of granulation tissue. In all other cases, no grossly denatured or birefringent collagen was noted within the granulation tissue.

By 9 days, all of the sites were free of crusts and showed only erythema on gross examination. Erythema resolved slowly over the next 3 weeks.

By 21 days, gross erythema was similar between the sites, and, microscopically the fibroplasia zones were not significantly different despite the early differences in thermal damage. These zones were comprised of large numbers of fibroblasts, with large nuclei admixed with numerous small vessels. The areas showed clear spaces consistent with mucin deposition.

After 42 days, treatment sites grossly resembled normal surrounding skin, and there was little variability in the appearance of the wounds. However, there was focal nodularity and whitening of the skin seen at sites 3, 4, 5, 8, 10, and 11. These areas showed 1–2-mm firm white nodules, and the pig's relaxed skin tension lines were intact except for these focal areas. No hypertrophic scarring was noted. Microscopically, the zones of fibroplasia were remarkably similar, with the stacked sites showing only slightly more fibroplasia. Compared to 21 days after treatment, all of the sites showed overall smaller fibroblast nuclei and absolute numbers of fibroblasts, and the number of vessels decreased. Also, there were focal regions with compaction of the fibroplasia zone with associated horizontal orientation of fibroblasts. Overall, however, most of the extracellular matrix (ECM) showed loose organization with randomly oriented collagen fibers. No microscopic changes consistent with hypertrophic scarring were noted, even in the deepest wounds. No statistically significant differences in fibroplasia thickness were noted between any of the sites (Table 5).

TABLE 5. Fibroplasia Zones (μm)

Site	21 days after surgery	42 days after surgery
1	168 ± 21	178 ± 16
2	210 ± 13	215 ± 21
3	180 ± 21	224 ± 25
4	207 ± 32	193 ± 32
5	220 ± 24	240 ± 17
6	174 ± 15	192 ± 14
7	162 ± 28	215 ± 35
8	240 ± 45	236 ± 31
9	172 ± 23	195 ± 27
10	191 ± 21	218 ± 27
11	225 ± 37	245 ± 40

DISCUSSION

Selective thermolysis in skin resurfacing differs from other laser applications. For tattoo particles and vascular structures, for example, wavelength and pulse durations are designed according to absorption spectra and sizes of discrete structures, where these targets comprise only a small fraction of the skin. The goal is relative sparing of the surrounding epidermis as well as the collagenous fibers and fibroblasts in the dermis [15]. In contrast, the target in skin resurfacing with infrared (IR) lasers is water, a ubiquitous tissue constituent. The goal is to restrict the pulse duration so that the bulk of the laser energy is confined to one optical penetration depth (OPD) of the incident energy. For CO_2 lasers in tissue, the OPD is about 20 μm, which corresponds to a thermal relaxation time of 0.5–1 msec based on commonly used time constant models. If energy is delivered in less than this time, heat diffusion is said to be limited during the laser pulse [15–18].

A popular concept in LSR is "ablation threshold." For the CO_2 laser in skin, it has been shown to be 3–8 J/cm^2 for millisecond domain pulses [19,20]. Most resurfacing CO_2 lasers operate at fluences just at or above threshold, so that only a

fraction of the energy is used for ablation; the majority is invested in heating of tissue water. This heat diffuses radially and forms concentric reproducible temperature zones that extend from the hot surface to the cooler periphery [16–18]. Thus, nonablative models can be used to characterize CO_2 LSR heating for typical fluences.

Thermal effects can be divided into low and high temperature processes. Low temperature processes (43–95°C) can generally be described by rate kinetics, and the pathologic changes are generally based on temperature–time categories, where damage has been shown to be exponentially dependent on temperature and linearly dependent on time. High temperature processes include water-dominated tissue vaporization (100°C+) and combustion, molecular disassociation, and plasma formation (300–1000°C) [21]. For LSR, exposures are much shorter than those formally characterized, and it is unknown if established rate constants continue to be valid for millisecond pulses. Most likely, much higher temperatures are required to duplicate the denaturation cascade of lower temperatures.

Long exposure and low temperature thermal injury typically cannot be seen immediately after heating by routine microscopy, and the first light microscopic evidence of injury is said to occur after 24 h [21]. This finding is consistent with our observations, where NBT staining was positive in the transition zone just after irradiation, whereas 24 hr later cell death was noted within this area. We found that this cell viability stain depth coincided within 10 μ with the depth of PMN margination. Thus, the PMNs appeared to accurately differentiate viable from dead cells after 1 day.

At higher temperatures (90–300°C), thermal coagulation of tissue is observed, defined as thermally induced irreversible changes of proteins and other biological molecules. Nonviable tissue coagulation (i.e., collagen) differs from low temperature injury in that it is seen immediately after treatment. One of the recognizable changes is loss of collagen birefringence [21]. For collagen denaturation, it has been shown that complete loss of birefringence occurred after 160 sec of heating at 73°C, but it cannot be assumed that these changes occur at temperatures this low after the instantaneous heating observed in pulsed laser irradiation [22]. Most likely, complete denaturation for short exposures (<1 msec) requires more than 100°C.

Tinctorial changes in collagen were found in our study to approximate the depths of injury as indicated by NBT staining and PMN line margination. However, with pulse stacking, there was a less distinct line between denatured and intact collagen, and there was a thicker transition zone than in those injuries produced by only one pulse or scan. Interestingly, the NBT stain depth from postoperative day 1 correlated well with the transition zone depth immediately after surgery so long as the deepest regions revealing any collagen changes were included in determining the depth of injury immediately after surgery.

If irradiation is repeated before tissue cools completely, temperature elevations will be additive. Moreover, if the repetition rate is rapid enough, then the temperature profile is similar to that of CW radiation [21–25]. The often cited 1-msec thermal relaxation time (τ_r) for the CO_2 laser is based on a calculated thermal diffusion constant. Based on this value for τ_r, repetition rates as high as 1,000 Hz ($1/\tau_r$) have been proposed as upper limits for avoiding cumulative heating between pulses. More conservative estimates of ~100 Hz were later predicted [26]. Venugopalan et al. [27] found that frequencies as high as 30 Hz could be used when one greatly exceeds ablation threshold and still avoid cumulative thermal damage.

Brugmans et al. [28] reported a much lower critical frequency for cumulative heating with subablative fluences. They noted that 5 Hz was the lowest frequency (200 msec cooling time) without considerable increases in RTD. Thus, caution should be exercised when interpreting τ_r based on time constant models because they only offer only an "order of magnitude picture" [29]. Thus, whereas τ_r determined by the time constant model describes temperature rises accurately, postpulse cooling is poorly characterized. The discrepancy stems from the time constant model not allowing for a change in the spatial distribution of temperature rise due to diffusion (i.e., the time constant model assumes the original spatial temperature distribution at the beginning and end of the pulse; this temperature decay is exponential, whereas the spatial extent remains constant). However, it has been shown that the temperature profile spreads in an axial direction, and the temperature decay thus becomes very slow with longer times [28]. In reality, heat conduction increases the characteristic length of the temperature change, and the heated volume increases during and after the pulse. Thus, the time "constant" is not truly constant but rather "time" dependent. Decay times for axial cooling actually

proceed according to $1/\sqrt{t}$, where t is the postpulse time interval. This "slower" cooling is consistent with our observations, where the interpusle time differed considerably and even times as long as 0.5 sec were associated with increased RTD [29,30].

Also, Welch et al. [31] found that elevated surface temperatures were noted even 250 msec after single pulses with CO_2 LSR. They found that 20–40 msec were required for cooling to 1/e of T_{MAX} and that ~500 msec were necessary for cooling to 10% of T_{MAX}. In a later article from this group [32], they concluded that pulse stacking undermines the beneficial effects of high-energy short-pulsed laser heating.

Another explanation for increased thermal damage with stacking is related to presumed changes in surface optical properties (i.e., not wiping between passes with stacking). Desiccation of even a very superficial layer of skin presumably allows additional laser passes to reach the deeper layers of skin before absorption and attenuation. However, because higher surface temperatures have been recorded in the absence of wiping between passes (even with 3 min between overlapping pulses), it is more likely that surface char decreases surface thermal conductivity and increases the absorption coefficient on the second and third passes [32]. With wiping and adequate time delays, we observed no increase in RTD, so that pass number per se did not independently increase RTD.

In this article, we have not rigorously analyzed heat conduction (or directly measured surface temperatures) as others have done, but have merely cited recent studies whose findings are consistent with ours. In these studies, approximations were made, for example by assuming that spot size was much greater than the OPD. Obviously, this is truer for the UltraPulse than for the SilkTouch system. Furthermore, scanning versus pulsed heating has not been rigorously compared for the CO_2 laser in LSR. There are many other complexities in performing a rigorous analysis of nonablative heat transfer in CO_2 LSR; for example, the CPG scans in an XY pattern so that the intervals between equidistant pulses will be different depending on whether they are across or down the line from one another.

The final wound appearances suggested no adverse effects from pulse stacking despite increased thermal damage. One reason is the nature of porcine skin wound healing after surface trauma. Pigs rarely develop hypertrophic scars, even after deep third-degree burns, and their skin is able to tolerate deeper injuries than the skin of humans without loss of the relaxed skin tension lines [33]. In another experiment, we observed loss of the relaxed skin tension lines in the skin of the pig only after dermabrading down to almost a millimeter, a depth almost certain to cause scarring in human skin. The threshold depth of injury for producing a scar in facial skin is unknown. Certainly it is site specific, the thin periorbital skin (dermis about 600 μm) being unable to tolerate the same depth of injury as thicker facial skin regions. Also, although the dermis over the mandible and upper lip is not as thin as that over the periorbital area (thickness is 800–1500 μm), these regions are most susceptible to hypertrophic scarring after any resurfacing procedure [34]. On biopsies we have performed in other human facial resurfacing studies, we encountered no significant scarring by restricting the level of necrosis to 200 μm into the dermis. Certainly if we were to allow for pulse stacking, this limit would be exceeded. We have noted clinically that in general (with the exception of the periorbital area) that making additional passes (up to three or four) does not prolong healing when each pass is made independently, probably because the thermal damage depth is the same, the only difference in the total depth of injury between passes being the slight dermal ablation depth per pass (about 10 μm for the UltraPulse at 7.5 J/cm^2). This has been shown nicely by Burkhardt and Maw [35] who noted no adverse sequelae with up to eight passes of the CO_2 laser so long as each pass was performed independently in time. With pulse stacking, however, the added depth of necrosis easily surpasses the ablation depth per pass, so that stacking is a likely a greater risk factor than pass number for scarring in human skin. Other potential contributors to scarring are wound infection, too many independent passes, and inadequate postoperative wound care. Clinicians are advised to exercise caution when using newer pulsed and scanning CO_2 systems. The exploitation of the designs of these devices demands that the laser settings and/or hand movements be precise and consistent so that heat accumulation is avoided.

ACKNOWLEDGMENTS

We thank Margaret E. Sherwood for LDH staining and Norm Michaud for the photographs.

REFERENCES

1. Apfelberg DB. The ultrapulse carbon dioxide laser with computer pattern generator automatic scanner for facial

cosmetic surgery and resurfacing. Ann Plast Surg 1996; 36:522–529.
2. Alster T. Comparison of two high-energy, pulsed carbon dioxide lasers in the treatment of periorbital rhytides. Dermatol Surg 1996;22:541–545.
3. Fitzpatrick R, Goldman M. Advances in carbon dioxide laser surgery. Clin Dermatol 1995;13:35–47.
4. Fitzpatrick R, Goldman M, Satur N, Tope W. Pulsed carbon dioxide laser resurfacing of photoaged skin. Arch Dermatol 1996;132:395–402.
5. Hruza GJ, Dover JS. Laser skin resurfacing [editorial; comment] [review]. Arch Dermatol 1996;132:451–455.
6. Hruza G. Skin resurfacing with lasers. Fitzpatrick's J Clin Dermatol 1995;3:38–41.
7. Lask G, Keller G, Lowe N, Gormley D. Laser skin resurfacing with the SilkTouch flashscanner for facial rhytides. Dermatol Surg 1995;21:1021–1024.
8. Lowe NJ, Lask G, Griffin ME. Laser skin resurfacing: pre- and posttreatment guidelines. Dermatol Surg 1995; 21:1017–1019.
9. Penoff J. Laser skin resurfacing. Ann Plast Surg 1996; 36:392–393.
10. Arnold D, Slatkine M, Zair E. Swiftlase: A new technology for char-free ablation in rectal surgery. J Clin Laser Med Surg 1993;11:309–311.
11. UltraScan™ Computer Pattern Generator Operator Manual, Coherent Laser Group, Palo Alto, CA, 1986: 1–18.
12. Lowe NJ, Lask G, Griffin ME, Maxwell A, Lowe P, Quilada F. Skin resurfacing with the Ultrapulse carbon dioxide laser. Dermatol Surg 1995;21:1025–1029.
13. David LM, Sarne AJ, Unger WP. Rapid laser scanning for facial resurfacing. Dermatol Surg 1995;21:1031–1033.
14. Hukki J, Lipasti J, Castren M, Puolakkainen P, Schröder T. Lactate dehydrogenase in laser incisions: a comparative analysis of skin wounds made with steel scalpel, electrocautery, superpulse-continuous wave carbon dioxide lasers, and contact Nd:YAG laser. Lasers Surg Med 1989; 9:590–594.
15. Anderson R, Parrish J. Selective photothermolysis: precise microsurgery by selective absorption of pulsed radiation. Science 1983;220:524–526.
16. Walsh J, Deutsch T. Pulsed CO2 laser ablation: measurement of the ablation rate. Lasers Surg Med 1988;8:264–275.
17. Walsh J, Flotte T, Anderson R, Deutsch T. Pulsed CO2 laser tissue ablation: Effect of tissue type and pulse duration on thermal damage. Lasers Surg Med 1988;8:108–118.
18. Venugopalan V, Nishioka NS, Mikic BB. The effect of laser parameters on the zone of thermal injury produced by laser ablation of biological tissue. J Biomed Eng 1994; 116:62–70.
19. Walsh JT Jr, Deutsch TF. Er:YAG laser ablation of tissue: measurement of ablation rates. Lasers Surg Med 1989;9:327–337.
20. Ross EV, Domankevitz Y, Skrobal M, Anderson RR. Effects of CO_2 laser pulse duration in ablation and residual thermal damage: implications for skin resurfacing. Lasers Surg Med 1996;19:123–129.
21. Thomsen S. Pathologic analysis of photothermal and photomechanical effects of laser-tissue interactions. Photochem Photobiol 1991;53:825–835.
22. Zweig A, Meieirhofer B, Muller O. Lateral thermal damage along pulsed laser incisions. Lasers Surg Med 1990; 10:262–274.
23. Venugopalan V, Nishioka N, Mikic B. The effect of laser parameters on the zone of thermal injury produced by laser ablation of biological tissue. ASME J Biomech Engin 1994;116:62–70.
24. Venugopalan V, Nishioka NS, Mikic BB. The effect of CO_2 laser pulse repetition rate on tissue ablation rate and thermal damage. IEEE Trans Biomed Eng 1991;38: 1049–1052.
25. Zweig A. A thermo-mechanical model for laser ablation. J Appl Phys 1991;70:1684–1691.
26. Van Gemert M, Welch A. Time constants in thermal laser medicine. Lasers Surg Med 1989;9:405–421.
27. Venugopalan V, Nishioka NS, Mikic BB. The effect of CO2 laser pulse repetition rate on tissue ablation rate and thermal damage. IEEE Trans Biomed Eng 1991;38: 1049–1052.
28. Brugmans M, Kemper J, Gijsber G, van der Meulen F, van Gemert M. Temperature response of biological materials to pulsed non-ablative CO2 laser irradiation. Lasers Surg Med 1991;11:587–594.
29. van Gemert M, Welch A. Approximate solutions for heat conduction: time constants. In: Welch A, van Gemert M, editors. Optical thermal response of laser-irradiated tissue. New York: Plenum; 1995. p 411–443.
30. van Gemert MJ, Lucassen GW, Welch AJ. Time constants in thermal laser medicine: II. Distributions of time constants and thermal relaxation of tissue. Phys Med Biol 1996;41:1381–1399.
31. Welch A, Chan E, Barton J, Choi B, Thomsen S. Infrared imaging of CO_2 laser resurfacing. Proc SPIE 1997;2970: 305.
32. Choi B, Barton J, Chan E, Thomsen S, Welch A. Infrared imaging of CO_2 laser ablation: implications for laser skin resurfacing. Proc SPIE 1998;3245:344–355.
33. Swindle M, Smith A, Hepburn B. Swine as models in experimental surgery. J Invest Surg 1988;1:65–79.
34. Stegman S, Tromovitch T, Glogau R. Cosmetic dermatologic surgery. 2nd ed. St. Louis: Mosby; 1990.
35. Burkhardt BR, Maw R. Are more passes better? Safety versus efficacy with the pulsed CO_2 laser. Plast Reconstr Surg 1997;100:1531–1534.